Received: 17 July 2024 | Revised: 9 January 2025 | Accepted: 13 January 2025

DOI: 10.1111/epi.18283

Epilepsia®

RESEARCH ARTICLE

Stereoelectroencephalographic exploration and surgical outcome in Lennox–Gastaut syndrome

Soomi Cho[1,2] | **Julia Makhalova**[1,3,4] | **Samuel Medina Villalon**[1,3] | **Nathalie Villeneuve**[5] | **Agnes Trébuchon**[1,3] | **Manel Krouma**[6] | **Didier Scavarda**[6] | **Anne Lépine**[5] | **Mathieu Milh**[5] | **Romain Carron**[1,3] | **Francesca Bonini**[1,3] | **Géraldine Daquin**[1] | **Sandrine Aubert**[1] | **Stanislas Lagarde**[1,3] | **Francesca Pizzo**[1,3] | **Fabrice Bartolomei**[1,3]

[1]Department of Epileptology and Cerebral Rhythmology, APHM, Timone Hospital, Marseille, France

[2]Department of Neurology, Severance Hospital, Yonsei University College of Medicine, Seoul, Republic of Korea

[3]Aix Marseille University, INSERM, Institute of Systems Neuroscience, Marseille, France

[4]Aix Marseille University, CNRS, CRMBM, Marseille, France

[5]Department of Pediatric Neurology, APHM, Timone Hospital, Marseille, France

[6]Department of Pediatric Neurosurgery, APHM, Timone Hospital, Marseille, France

Correspondence
Fabrice Bartolomei, Service d'Epileptologie et de Rythmologie Cérébrale, Hôpital Timone, 264 Rue Saint-Pierre, Marseille 13005, France.
Email: fabrice.bartolomei@ap-hm.fr

Abstract

Objective: Lennox–Gastaut syndrome (LGS) is typically characterized by drug-resistant epilepsy and subsequent cognitive deterioration. Surgery is a rare but viable option for the control of seizures in a subset of patients with LGS. This study aimed to describe the organization of the epileptogenic zone network (EZN) in patients with LGS using stereoelectroencephalography (SEEG) and to report the outcome of post-SEEG treatment.

Methods: A quantitative SEEG signal analysis was conducted in 14 consecutive patients with LGS, in whom a potentially localized EZN was suggested based on a comprehensive noninvasive evaluation. The EZN and the irritative zone network were identified using relevant biomarkers during ictal (epileptogenicity index and connectivity epileptogenicity index) and interictal (spikes and high-frequency oscillations) recordings. The applied post-SEEG treatments were assessed, including SEEG-guided radiofrequency thermocoagulation (RF-TC), surgery, and neurostimulation.

Results: The seizure onset patterns showed some specificity by seizure type, with 84% of tonic seizures involving low-voltage fast activity. The EZN of patients with LGS was often, but not always, complex and extensive, involving two or more lobes (79%) and both hemispheres (64%). The lateral neocortical structures, particularly the lateral premotor and dorsolateral prefrontal cortices, were identified as being most frequently involved in the EZN. Among the explored subcortical structures, only the pulvinar, central–lateral thalamic nucleus, and hypothalamic hamartoma belonged to the EZN. Twelve patients (86%) underwent SEEG-guided RF-TC, with 50% experiencing a >50% reduction in baseline seizure frequency. Four patients (29%) underwent curative

surgery for significant involvement of a lesion in the EZN, and one case achieved an Engel class I outcome.

Significance: This is the first quantitative SEEG study in patients with LGS to demonstrate the utility of SEEG in identifying patients who may benefit from surgery and to perform SEEG-guided RF-TC. Nevertheless, the indications for SEEG should be carefully assessed, as localized EZN is uncommon in LGS.

KEYWORDS

epileptogenic zone, epileptogenicityLGSpost-SEEG outcome, SEEG

1 | INTRODUCTION

Lennox–Gastaut syndrome (LGS) is a developmental and epileptic encephalopathy that exhibits distinct clinicoelectrical features.[1–3] Clinically, LGS typically begins in childhood and is characterized by tonic seizures and at least one other type of seizure, along with intellectual disability. Electroencephalographically, generalized slow spike-and-wave complexes (SSW) at ≤2.5 Hz and generalized paroxysmal fast activity (GPFA) are the typical interictal patterns of LGS.

LGS is generally drug-resistant, and persistent seizures are associated with cognitive, behavioral, and psychiatric impairment that may worsen over time. On the other hand, it has been suggested that neurological and neuropsychological function may be fully or partially restored after a period of seizure freedom (SF) or reduced seizure frequency.[4–9] Therefore, seizure control is crucial and may require combining various treatment strategies. Nonpharmacologic therapeutic options for LGS include a ketogenic diet, corpus callosotomy, neurostimulation, radiofrequency thermocoagulation (RF-TC), and resective surgery.[10]

Surgical resection is unlikely to be indicated in most patients with LGS. However, it can be effective and even curative for some selected patients.[7,9] Stereoelectroencephalography (SEEG) is an effective method for identifying the epileptogenic zone (EZ) and eloquent areas, evaluating the feasibility of surgical resection, and performing SEEG-guided RF-TC.[11] However, there have been few studies on the use of intracranial electroencephalography (EEG) in patients with LGS,[12–15] and none has quantified the SEEG signal to delineate the EZ network (EZN).

This study aimed to describe the SEEG findings and subsequent surgical decisions in patients with LGS. The degree of involvement of various cortical structures and the individual EZN organization were quantified using the epileptogenicity index (EI) and connectivity EI (cEI). Moreover, post-SEEG treatments and outcomes were investigated.

Key points

- The epileptogenic networks of LGS were widely distributed and often involved bilateral frontal regions, as demonstrated by SEEG analysis.
- Despite high interindividual variability across seizures, EZN organization was consistent according to seizure type.
- Only a minority of LGS patients explored by SEEG were ultimately eligible for curative surgery.
- Quantification of SEEG may assist in guiding individual surgical strategy and radiofrequency thermocoagulation targets in LGS.

2 | MATERIALS AND METHODS

2.1 | Patient selection

A total of 14 consecutive patients with LGS identified from a database of >500 surgical candidates who underwent SEEG exploration between January 2005 and December 2023 at Timone Hospital (Marseille, France) were included in the study. The diagnosis of LGS was based on key characteristics outlined by Gastaut et al. in 1966 and the International League Against Epilepsy taskforce.[1,3] We included all patients who exhibited the following characteristics: (1) tonic seizures plus at least one of the following seizures: atonic and atypical absences, (2) diffuse EEG abnormalities (SSW and GPFA), and (3) mild to profound intellectual disability.

All patients underwent bilateral and systematic SEEG exploration if a focal etiology of LGS could be presumed based on converging evidence from noninvasive assessments, including seizure semiology, scalp video-EEG, 1.5- or 3-T magnetic resonance imaging (MRI), fluorodeoxyglucose positron emission tomography, and

magnetoencephalography. Detailed clinical history, neurological examination, and neuropsychological testing were reviewed during the SEEG recordings. Pre-SEEG clinical data, SEEG recordings, pre- and postimplantation imaging, and post-SEEG treatment outcomes were collected.

All patients have given informed written consent, and the study was approved by the Assistance Publique–Hôpitaux de Marseille (health data access portal registration number PADS 5LNZWU).

2.2 | SEEG recordings

SEEG recordings were performed as part of routine presurgical assessment according to the French guidelines.[16] Intracerebral multiple contact electrodes (10–18 contacts with length = 2 mm, diameter = .8 mm, and 1.5 mm apart, Alcis or Dixi) were implanted stereotaxically.[17] The electrodes were anatomically targeted for each patient based on clinical hypotheses regarding the localization of the EZ, as determined by information from phase 1 evaluation. Table S1 provides detailed information on the sampled brain regions for each patient. The positions of electrodes were reconstructed using postimplantation computerized tomography (CT), which also allowed for the exclusion of intracranial bleeding. Signals were recorded on a Natus system and sampled at 512 or 1024 Hz with 16-bit resolution. A high-pass filter with a cutoff frequency of .16 Hz at −3 dB was used to eliminate very slow variations that sometimes contaminate the baseline.

2.3 | SEEG signal analysis

Signal analyses were performed in a bipolar montage and computed using open-source AnyWave software, available at https://meg.univ-amu.fr/wiki/AnyWave.[18]

For ictal recordings, visual analysis of the seizure onset pattern (SOP) and computation of the EI and cEI were performed. The SOP was visually analyzed without software filters and assessed on the earliest involved electrodes. The EI and cEI were computed from SEEG signals to quantitatively evaluate the degree of epileptogenicity and to identify the regions involved in seizure generation. Previous papers have described the methodologies for EI and cEI.[19,20] In brief, the EI combines the analysis of both spectral (the redistribution of signal energy from low-frequency [4–12 Hz] to high-frequency bands [12–127 Hz]) and temporal (the relative timing of this frequency redistribution across channels) domains.[19] The cEI combines the original EI with a directed connectivity measure ("out-degrees" in beta band).[20] The use of cEI allows better performance in quantifying slow SOPs (<12 Hz) without low-voltage fast activity (LVFA), which is difficult to achieve with EI. The EI and cEI were calculated simultaneously using a dedicated MATLAB plug-in (the cEI plug-in, https://meg.univ-amu.fr/wiki/AnyWave:Plug-ins). A minimum of three spontaneous seizures (at least one per seizure type if multiple seizure types were recorded) per patient were analyzed by an epileptologist (S.C.) and then discussed with two senior epileptologists (J.M. and F.Ba.).

Visual analysis and automatic detection of spikes and high-frequency oscillations (HFOs; 80–300 Hz) were performed for interictal recordings. Spikes and HFOs were quantified for each bipolar channel, and the maximal normalized rate per minute was computed using the Delphos (Detector of Electrophysiological Oscillations and Spikes) detector.[21] As previously described, a total of six 5-min interictal recordings were used for each patient: three during awake resting state and three during non-rapid eye movement sleep.[22] All 5-min datasets were obtained from two contiguous hours of wakefulness or two contiguous hours of sleep and were of good quality, with minimal artifacts and visually observed interictal epileptiform activity.

A previous study established cutoff values for the EI and cEI to identify SEEG-recorded structures as belonging to the EZN.[22] Brain structures with an EI ≥ .4 and/or a cEI ≥ .65 were identified as belonging to the EZN. The propagation zone network (PZN) was defined as contacts with .1 < EI < .4 and/or .3 < cEI < .65 and sustained discharge during the seizure. All other contacts were defined as noninvolved (NI). To determine the irritative zone network (IZN) where interictal epileptic discharges are generated, the cutoffs of .48 and .38 were used for the maximal normalized spike and HFO rates, respectively, based on the previous study.[22]

2.4 | Region of interest definition

In each patient, automated anatomical localization and labeling of each electrode contact was conducted using Gardel software (EpiTools software suite), which is accessible at https://meg.univ-amu.fr/wiki/GARDEL:presentation. The preimplantation T1-weighted MRI was coregistered with the postimplantation CT images, followed by automatic identification and anatomical localization of each electrode contact. Coregistration was then performed with the Virtual Epileptic Patient (VEP) atlas for automated brain parcellation (available at https://ins-amu.fr/vep-atlas),[23] in conjunction with the 7TAMIbrain$_{DGN}$ atlas for automated parcellation of thalamic nuclei and basal ganglia.[24] Each contact was automatically assigned to the respective anatomical region of the combined atlas (75 cortical regions and 24 deep gray nuclei per hemisphere, including 12 thalamic nuclei, obtained through the implementation of an in-house FreeSurfer-based segmentation pipeline) projected in the patient's MRI space. Figure S1 illustrates the visualization

of the electrodes located in different thalamic nuclei within the patient's anatomy. Each brain region was then labeled as EZN, PZN, or NI (for EI or cEI), or as IZN or non-IZN (for spikes and HFOs), based on the definition used for the bipolar contacts that sampled the respective regions, as described above. If a region was sampled by two or more bipolar contacts, the maximum values of the respective ictal or interictal epileptogenicity markers obtained for this region were used. Finally, to perform group analyses of epileptogenicity profiles in this small cohort of patients, we regrouped the regions obtained by automated parcellation into 23 cortical and eight subcortical regions per hemisphere (see Table S1).

2.5 | Post-SEEG treatments and outcome assessments

Nonpharmacological treatment approaches used after SEEG were investigated, including SEEG-guided RF-TC, resective surgery, corpus callosotomy, vagus nerve stimulation (VNS), and deep brain stimulation (DBS). The criteria for selecting SEEG contacts for RF-TC have been previously reported.[25,26] Briefly, contacts were considered eligible for RF-TC if they belonged to the EZN and/or were located in an MRI-visible lesion suspected to be epileptogenic. Contacts within the eloquent cortex or deemed too close to vascular structures were excluded from RF-TC. The number of targeted contacts and SF duration after RF-TC were evaluated. For surgical resection, type of surgery, surgical outcomes using Engel's classification, and SF duration after surgery were assessed. Clinical response to RF-TC, callosotomy, VNS, and DBS was defined as a 50% or greater reduction in the baseline seizure frequency. It was assessed at the last follow-up or before any subsequent nonpharmacological treatment started.

2.6 | Statistical analysis

Data are presented as mean (SD) or median (interquartile range [IQR]) for continuous variables and number (percentage) for categorical variables. For nonparametric data, continuous variables were compared using the Mann–Whitney *U*-test.

3 | RESULTS

3.1 | Patient characteristics

The clinical characteristics of the 14 included patients are summarized in Table 1. The cohort consisted of eight male and six female patients, with median age at epilepsy onset of 1.8 years (IQR = .5–3.5, range = .1–14.0). At the onset of epilepsy, seven patients (50%) were diagnosed with LGS, four (29%) with focal epilepsy, two (14%) with West

TABLE 1 Clinical characteristics of study population.

Characteristic	Value
Sex, *n* (%)	
Male	8 (57)
Female	6 (43)
Age at epilepsy onset, years [IQR; range]	1.8 [.5–3.5; .1–14.0]
Diagnosis at epilepsy onset, *n* (%)	
Lennox–Gastaut syndrome	7 (50)
Focal epilepsy	4 (29)
West syndrome	2 (14)
Idiopathic generalized epilepsy	1 (7)
Age at SEEG, years [IQR; range]	11.5 [10.0–21.8; 4.0–30.0]
Cognitive status at SEEG, *n* (%)	
Mental retardation [IQ < 70]	12 (86)
Mild cognitive involvement	2 (14)
Family history of seizure, *n* (%)	0 (0)
Seizure type, *n* (%)	
Tonic seizure with asymmetric manifestation	4 (100)
Focal aware and/or focal impaired awareness seizure	11 (79)
Atonic seizure	10 (71)
Atypical absence seizure	7 (50)
MRI findings, *n* (%)	
Normal	5 (36)
Malformations of cortical development	5 (36)
Focal cortical dysplasia	3 (21)
Polymicrogyria	1 (7)
Schizencephaly, polymicrogyria, and multiple heterotopias	1 (7)
Hypothalamic hamartoma	2 (14)
Hemispheric atrophy	1 (7)
Temporal pole arachnoid cyst	1 (7)
Interictal scalp EEG findings, *n* (%)	
Generalized slow spike–wave	14 (100)
Focal or multifocal interictal epileptiform discharges	14 (100)
Generalized paroxysmal fast activity	12 (86)
Background slowing	13 (93)

Abbreviations: EEG, electroencephalographic; IQ, intelligence quotient; IQR, interquartile range; MRI, magnetic resonance imaging; SEEG, stereoelectroencephalography.

syndrome, and one (7%) with idiopathic generalized epilepsy. The latter diagnosis has been revised and changed to focal epilepsy based on the scalp video-EEG electroclinical data. The median age at SEEG was 11.5 years (IQR = 10.0–21.8, range = 4.0–30.0). Neuropsychological assessment at the time of SEEG revealed that 12 patients (86%) had mental retardation (intelligence quotient [IQ] < 70), and two patients (14%) had mild cognitive impairment (IQ between 70 and 80). None of the patients had a family history of epilepsy.

Electroclinical, MRI, and SEEG data are presented in Table 2. All 14 patients had tonic seizures with asymmetric features, such as a tonic posture predominantly affecting one arm or a head version. Eleven patients (79%) had focal aware seizures (FAS) and/or focal impaired awareness seizures (FIAS), 10 (71%) had atonic seizures, and seven (50%) had atypical absences. Brain MRI was normal in five patients (36%). Of the nine cases with abnormal MRI findings, five (36%) had malformations of cortical development, including focal cortical dysplasia (FCD; three cases, 21%), polymicrogyria (one case, 7%), and schizencephaly with polymicrogyria and multiple heterotopias (one case, 7%), two (14%) had hypothalamic hamartoma (HH), one (7%) had hemispheric atrophy, and one (7%) had an arachnoid cyst. In all 14 patients, generalized SSW and focal interictal epileptiform discharges were observed on scalp EEG. GPFA was seen in 12 patients (86%) as purely subclinical discharges. In the two remaining patients, these brief discharges were associated with slight tonic axial contraction. Background slowing was present in 13 patients (93%).

3.2 | Electroclinical features according to the seizure type

Sixty-nine seizures (38 tonic, 14 FAS/FIAS, nine atonic, and eight atypical absences) were analyzed. Table 2 presents the results of a visual analysis of the SOPs for each patient and seizure type.

Twelve of 14 patients (86%) had an SOP characterized by LVFA preceded or not by slow-wave direct current (DC) shift, preictal spiking, or a burst of polyspikes in at least one seizure. The SOPs showed some specificity of the electrical signature according to the seizure type. In particular, 84% (32/38) of tonic seizures disclosed a pattern of LVFA with or without preceding transitional features (Figure 1A). Nevertheless, the anatomoelectroclinical correlations were difficult, and both tonic and atonic phenomena could be observed with the same distinctive SOP at the individual patient level. Among the tonic seizures, some brief spasmlike seizures exhibited an SOP of brief LVFA discharge superposed on a high-amplitude slow wave. The same SOP was a signature of atonic seizures in the same patient (Figure 1B). Furthermore, the SOP of 44% of atonic seizures exhibited a slow-wave DC shift, which was followed by more sustained LVFA. This pattern was also observed in tonic seizures. The main onset pattern of atypical absences (7/8, 88%) was characterized by slow rhythmic spike–waves at 1–2 Hz over widely distributed regions (Figure 1C). FAS and/or FIAS exhibited regional ictal onsets with various SOPs, as previously described in focal epilepsies.[27] Additionally, the widespread interictal spikes were diminished at the onset of the seizures (Figure 1D). The number and extent of anatomical regions involved in the EZN exhibited some variation between different seizure types in a patient and even within the same seizure type. However, no distinct network topographies were identified according to the seizure type within a patient.

Figure 2 shows an illustrative case where SEEG analysis identified a localized, temporal EZN, and a tailored resection was performed, resulting in an excellent surgical outcome (Engel class I).

3.3 | Organization of the epileptogenic network

Detailed results of ictal epileptogenicity levels (EZN, PZN, or NI) of the explored brain regions among the 23 cortical regions of interest (ROIs; as defined by the VEP atlas) and eight subcortical ROIs (as defined by the 7TAMIbrain$_{DGN}$ atlas), including the pulvinar, mediodorsal, central–lateral, and lateral thalamic nuclei, caudate nucleus, putamen, pallidum, and HH with adjacent hypothalamus, are shown in Table S1. The mean number of anatomical regions for which the EI and/or cEI were quantified in each patient was 37.4 ± 10.4 (range = 16.0–52.0). The EZN of the patients with LGS was often, but not always, widely distributed in both lesional and nonlesional cases. The EZN implicated two or more lobes in 79% (11/14) of cases and both hemispheres in 64% (9/14) of cases (Table 2). The EZN most commonly involved the frontal lobe (12 cases, 86%), followed by the parietal lobe (six cases, 43%), temporal lobe and insula (five cases, 36% each), and occipital lobe (three cases, 21.3%).

The prevalence of involvement of cortical and principal subcortical regions in the EZN and the IZN, controlled for the number of times each structure was sampled, is shown in Figure 3A. Except HH, for which SEEG sampling was performed only in the presence of lesions, the lateral neocortical structures, particularly the lateral premotor and dorsolateral prefrontal cortices, were identified as being most frequently involved in the

TABLE 2 Clinical, MRI, and SEEG characteristics of the patients.

Patient	Age at epilepsy onset, years	Seizure types	Possible focal semiological features	MRI findings	Scalp EEG findings	Age at SEEG, years	Depth electrodes/ analyzed contacts, *n*	SEEG seizure onset pattern (seizure type/ seizures analyzed, *n*)	EZN	Thal in EZN (involved nuclei)	EZN regions, *n*	EZN topography	IZN	IZN regions, *n*
P1	1.2	TS + FS + AS	Cephalic heating sensation; asymmetric tonic posturing	Normal	SSW + FIED + GPFA + AB	17	13 (R8, L5)/104	LVFA w/wo slow-wave DC shift (TS/3)	M1 (R), PMM (L), PML (B)	NA	4	Central–premotor (B)	M1 (B), PML (B), PMM (L), ACC (R), VLPFC (R), SPLmes (L)	8
P2	.3	TS + AA	Head version to L	Normal	SSW + FIED + GPFA + AB	21	10 (R6, L4)/92	LVFA w slow-wave DC shift (TS/3); rhythmic SSW (AA/2)	PML (B), PMM (R), DLPFC (B), DMPFC (R), ACC (B)	NA	8	Premotor–prefrontal (R > L)	PML (R), PMM (B), DLPFC (B), ACC (B), SPLlat (R)	8
P3	.1	TS + FS + AS + AA	R facial contraction	HH	SSW + FIED + GPFA + AB	4	10 (R1, L9)/113	High-amplitude slow-wave DC shift w superimposed LVFA (TS/2; AS/2); slow-wave DC shift followed by LVFA (TS/1); rhythmic polyspikes (FS/2)	HH (L), DLPFC (B), PML (L), PMM (L), M1 (L), PCC (L), IPL (L)	NA	8	HH and prefrontal–premotor–P (L > R)	HH (L), DLPFC (B), VLPFC (L), OFC (L), PML (L), TLant (L), PCC (L), IPL (L)	9
P4	14	TS + FS + AS	Throbbing sensation in LA; asymmetric tonic posturing; myoclonic jerks of LA; postictal LA deficits	Normal	SSW + FIED + GPFA	24	13 (R12, L1)/126	LVFA (TS/3; FS/1)	DLPFC (R), VLPFC (R), ACC (R), PML (R), PMM (R), M1 (R), PO (R), INSant (R), INSpost (R), IPL (R), Thal-Pu (R), Thal-CL (R)	Yes (Pu, CL)	12	Prefrontal–premotor–central–INS (R)	DLPFC (B), VLPFC (R), ACC (R), DMPFC (R), M1 (R), PML (R), PMM (R), PO (R), INSant (R), INSpost (R), Thal-Pu (R), Thal-CL (R)	13
P5	3	TS + FS + AS	Ascending heating sensation; asymmetric tonic posturing w/ wo "chapeau de gendarme"	Centro-P FCD, L	SSW + FIED + GPFA + AB	24	11 (R2, L9)/123	Preictal spiking followed by LVFA (TS/3); LVFA w/ wo slow-wave DC shift (TS/1; AS/1)	M1 (L), PML (L), PMM (B), IPL (L), SPLlat (L), PCC (L)	NA	7	Central–premotor–P (L > R)	M1 (L), PML (B), PMM (B), DLPFC (L), VLPFC (L), ACC (L), PO (L), INSant (L), SPLlat (L), SPLmes (B), IPL (L)	14
P6	1.1	TS + FS + AS	Vertigo; asymmetric tonic posturing	Normal	SSW + FIED + GPFA + AB	16	16 (R3, L13)/145	LVFA w/wo slow-wave DC shift (TS/3; AS/1)	DLPFC (B), DMPFC (L), VLPFC (L), OFC (L), PML (L), PMM (L), TLant (L), INSant (L), IPL (L), SPLlat (B)	NA	12	Prefrontal–premotor–P–INS (L > R)	DLPFC (B), DMPFC (L), VLPFC (L), OFC (L), PML (B), INSant (L), TLant (L), IPL (L), SPLlat (B), SPLmes (L)	13

TABLE 2 (Continued)

Patient	Age at epilepsy onset, years	Seizure types	Possible focal semiological features	MRI findings	Scalp EEG findings	Age at SEEG, years	Depth electrodes/ analyzed contacts, *n*	SEEG seizure onset pattern (seizure type/ seizures analyzed, *n*)	EZN	Thal in EZN (involved nuclei)	EZN regions, *n*	EZN topography	IZN	IZN regions, *n*
P7	1.5	TS + FS + AA	Indescribable feeling; oroalimentary automatism; asymmetric tonic posturing; myoclonic jerks of L face	T FCD, R	SSW + FIED + GPFA + AB	10	15 (R12, L3)/161	Preictal spiking followed by slow-wave DC shift and sharp alpha activity (FS/3)	TMant (R), TLant (R), VLPFC (R), OFC (R), Thal-Pu (R)	Yes (Pu)	5	Mesiolateral T–prefrontal (R)	TMant (B), TLant (R), TLpost (R), DLPFC (R), VLPFC (R), PCC (R)	7
P8	2	TS + FS + AA	Oroalimentary automatism; asymmetric tonic posturing w/wo head version to L	Normal	SSW + FIED + GPFA + AB	10	16 (R4, L12)/159	Slow-wave DC shift followed by LVFA (TS/2); rhythmic SSW (AA/3)	PML (B), M1 (R), DLPFC (B), VLPFC (L), DMPFC (B)	NA	8	Premotor–prefrontal–opercular (L > R)	PML (B), DLPFC (B), VLPFC (L), DMPFC (B), VMPFC (L), OFC (B), INSant (L), TMant (L), TLant (L)	13
P9	.3	TS + AS	Asymmetric tonic posturing	Hemispheric atrophy, L	SSW + FIED + GPFA + AB	10	15 (R2, L13)/156	LVFA w/wo slow-wave DC shift (TS/2; AS/2)	PML (L), M1 (L), DLPFC (L), VLPFC (L), OFC (L), DMPFC (L), ACC (L)	No	7	Premotor–prefrontal–central (L)	PML (L), PMM (L), DLPFC (L), VLPFC (L), INSpost (L), TLant (L), TLpost (L), S1 (L)	8
P10	5	TS + FS + AS + AA	Ascending abdominal heat; tingling sensation in head; oroalimentary and gestural automatism; head and eyes to L	HH	SSW + FIED + GPFA + AB	9	15 (R10, L5)/160	Polyspike–slow-wave DC shift (TS/2; AS/3); rhythmic polyspikes followed by slow-wave DC shift w/ wo LVFA (TS/2); rhythmic SSW (AA/2)	HH (R), PML (B), DLPFC (R), VLPFC (L), OFC (L), INSpost (L), IPL (R)	No	8	HH and premotor–prefrontal–P (B)	HH (R), PML (B), PMM (R), DLPFC (R), DMPFC (R), TLant (R), TLpost (R), IPL (R), SPLlat (R)	10
P11	3	TS + FS + AS	Indescribable feeling; oroalimentary automatism; head and eyes to L; asymmetric tonic posturing; postictal aphasia	T FCD, L	SSW + FIED + GPFA + AB	12	18 (R2, L16)/168	Preictal spiking followed by LVFA w/wo slow-wave DC shift (FS/2); LVFA w/wo slow-wave DC shift (TS/2; FS/2)	TMant (L), TMpost (L), TLant (L), TLpost (L), TB (L), OL (L)	No	6	Mesiolateral T–O (L)	TMant (L), TMpost (L), TLant (L), TLpost (L), OFC (L), OM (L), OL (L), IPL (L)	8

(Continues)

TABLE 2 (Continued)

Patient	Age at epilepsy onset, years	Seizure types	Possible focal semiological features	MRI findings	Scalp EEG findings	Age at SEEG, years	Depth electrodes/ analyzed contacts, *n*	SEEG seizure onset pattern (seizure type/ seizures analyzed, *n*)	EZN	Thal in EZN (involved nuclei)	EZN regions, *n*	EZN topography	IZN	IZN regions, *n*
P12	3	TS + FS + AS + AA	R hand automatism; asymmetric tonic posturing w/wo head and eyes to R	Schizencephaly, PMG, periventricular heterotopias, R	SSW + FIED + GPFA + AB	11	15 (R14, L1)/150	Burst of polyspikes followed by LVFA (FS/1); LVFA w/ wo slow-wave DC shift (TS/3)	M1 (R), PML (R), PMM (R), VLPFC (R), TLpost (R), INSant (R), INSpost (R), PO (R), IPL (R), SPLlat (R), OM (R)	No	11	Hemispheric involvement (R)	M1 (R), PMM (R), TLpost (R), TMpost (R), INSant (R), INSpost (R), PO (R), IPL (R), SPLlat (R), PCC (R), OM (R), Thal-LT (R)	12
P13	.6	TS + FS + AS + AA	Indescribable feeling; asymmetric tonic posturing	T–P INS PMG, L	SSW + FIED + GPFA + AB	11	21 (R4, L17)/177	LVFA w/wo slow-wave DC shift (TS/1; FS/3); slow-wave DC shift–LVFA followed by rhythmic SSW (AA/1)	PO (L), TLpost (L), TMant (L), IPL (L), SPLlat (L), SPLmes (L), PCC (L), OL (L), Thal-CL (L)	Yes (CL)	9	Mesiolateral T–P–O (L)	M1 (L), PML (L), TLant (B), TMant (B), TLpost (L), INSpost (L), PO (L), IPL (B), SPLlat (L), SPLmes (L), PCC (L), OL (L), OM (L)	16
P14	7	TS + MS	Asymmetric tonic posturing w head and eyes to L and "chapeau de gendarme"	T pole arachnoid cyst, L	SSW + FIED + GPFA + AB	30	14 (R3, L11)/138	Burst of polyspikes followed by LVFA (TS/3); LVFA w/ wo slow-wave DC shift (TS/2)	PML (B), DLPFC (B), VLPFC (L), OFC (L), DMPFC (B), TMant (L), TLant (L), INSant (L), INSpost (L), IPL (L), PCC (L)	No	14	Premotor–prefrontal–T–INS (L > R)	PML (B), DLPFC (B), VLPFC (L), OFC (L), DMPFC (L), TMant (L), TLant (L), TLpost (L), INSant (L), INSpost (L), PO (L), Thal-Pu (L)	14

Abbreviations: AA, atypical absence; AB, abnormal background; ACC, anterior cingulate cortex; AS, atonic seizure; B, bilateral; CL, central–lateral nucleus; DC, direct current; DLPFC, dorsolateral prefrontal cortex; DMPFC, dorsomedial prefrontal cortex; EEG, electroencephalographic; EZN, epileptogenic zone network; FCD, focal cortical dysplasia; FIED, focal interictal epileptiform discharge; FS, focal aware and/or focal impaired awareness seizure; GPFA, generalized paroxysmal fast activity; HH, hypothalamic hamartoma; INS, insula; INSant, anterior INS; INSpost, posterior INS; IPL, inferior parietal lobule; IZN, irritative zone network; L, left; LA, left arm; LT, lateral nucleus; LVFA, low-voltage fast activity; M1, primary motor; MRI, magnetic resonance imaging; MS, myoclonic seizure; NA, not applicable; O, occipital; OFC, orbitofrontal cortex; OL, lateral occipital; OM, mesial occipital; P, parietal; PCC, posterior cingulate cortex; PMG, polymicrogyria; PML, lateral premotor; PMM, mesial premotor; PO, parietal operculum; Pu, pulvinar; R, right; S1, primary sensory; SEEG, stereoelectroencephalographic; SPLlat, lateral superior parietal lobule; SPLmes, mesial superior parietal lobule; SSW, generalized slow spike–wave complexes; T, temporal; TB, temporal basal cortex; Thal, thalamus; TLant, anterior lateral temporal; TLpost, posterior lateral temporal; TMant, anterior mesial temporal; TMpost, posterior mesial temporal; TS, tonic seizure; VLPFC, ventrolateral prefrontal cortex; VMPFC, ventromesial prefrontal cortex; w, with; wo, without.

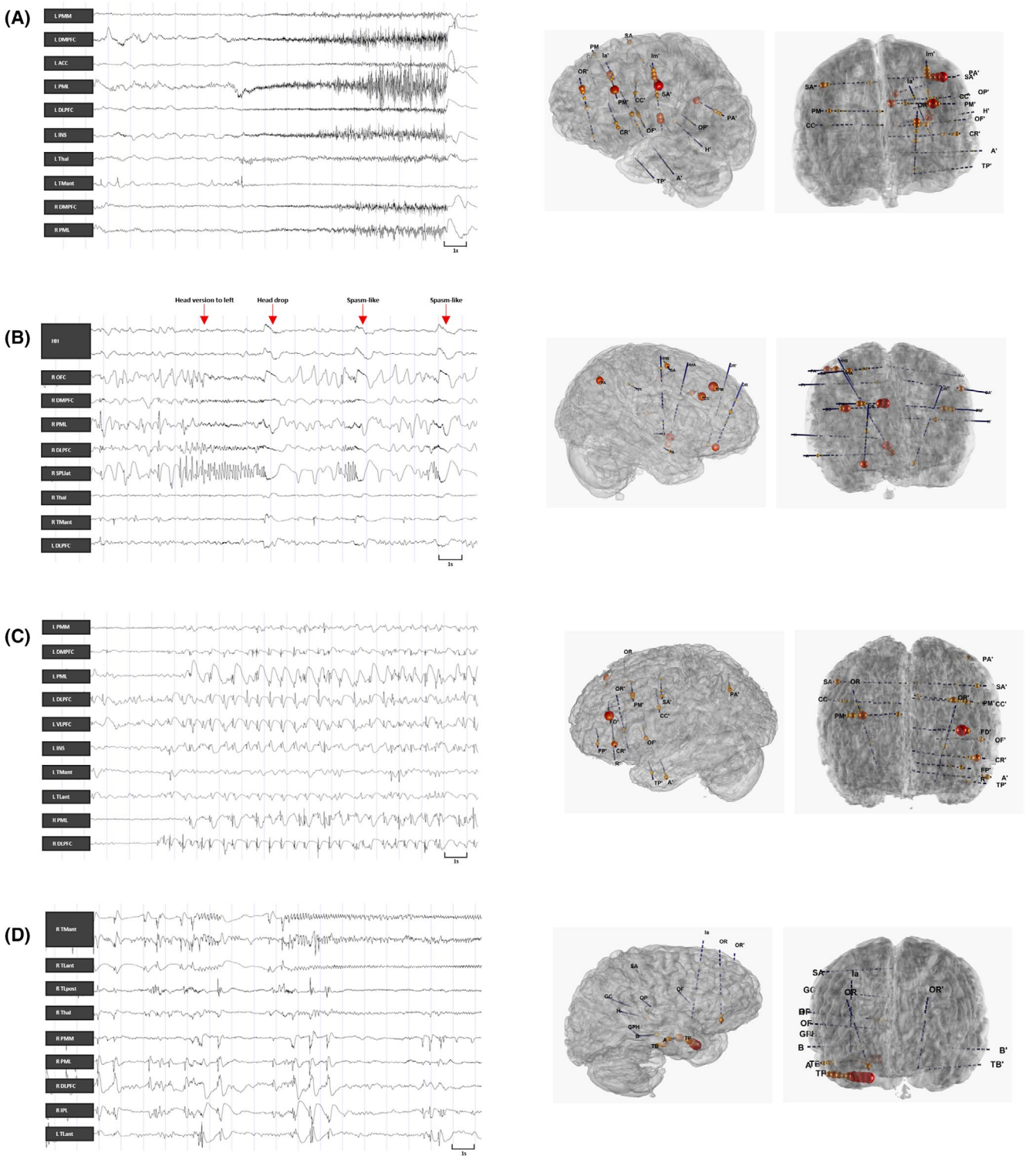

FIGURE 1 Legend on next page.

EZN. The lateral occipital regions were included in the EZN in two of only three cases with occipital sampling, which precludes the drawing of robust conclusions about their involvement at the group level. The IZN was observed to encompass a more extensive area of the brain and to involve a greater number of brain regions than the EZN in the majority of patients. The lateral premotor, dorsolateral prefrontal, parietal operculum, and anterolateral temporal cortices were frequently engaged as part of the IZN.

The organization of the EZN at the individual level was highly variable among the patients with LGS (Figure 3B) despite the shared scalp EEG features (i.e., generalized SSW and/or GPFA). In all patients, including those with

FIGURE 1 Examples of the seizure onset patterns (SOPs; left column) and three-dimensional representations of epileptogenicity index or connectivity epileptogenicity index to describe the epileptogenic zone network (EZN; right column) for each seizure type in Lennox–Gastaut syndrome patients. (A) Patient 06. Tonic seizure began with low-voltage fast activity (LVFA). The EZN involved a distributed, bilateral premotor–prefrontal–parietal network. (B) Patient 10 with hypothalamic hamartoma (HH). A cluster of seizures began with a tonic head version, followed by an atonic (head drop) seizure and then two brief tonic (spasmlike) seizures, all with a similar SOP characterized by a brief LVFA discharge superimposed on a high-amplitude slow wave. The EZN involved the premotor–prefrontal–parietal network as well as the HH. (C) Patient 08. Atypical absence seizure was characterized by slow rhythmic spike–wave discharge at 1–2 Hz. The EZN involved bilateral prefrontal and left premotor–opercular regions. (D) Patient 07 with right temporal focal cortical dysplasia. Focal impaired awareness seizures were characterized by preictal spiking followed by rhythmic sharp alpha activity over the right temporal region. The EZN mainly involved the right temporal lobe, with some epileptogenicity within the ipsilateral orbitofrontal cortex. L PMM, left premotor medial cortex; L DMPFC, left dorsomedial prefrontal cortex; L ACC, left anterior cingulate cortex; L PML, left premotor lateral cortex; L DLPFC, left dorsolateral prefrontal cortex; L INS, left insula; L Thal, left thalamus; L TMant, left temporomedial anterior; R DMPFC, right dorsomedial prefrontal cortex; R PML, right premotor lateral cortex; HH, hypothalamic hamartoma; R OFC, right orbitofrontal cortex; R DMPFC; right dorsomedial prefrontal cortex; R PML, right premotor lateral cortex; R DLPFC, right dorsolateral prefrontal cortex; R SPLlat, right superior parietal lobule lateral; R Thal, right thalamus; R TMant, right temporomedial anterior cortex; R DLPFC, right dorsolateral prefrontal cortex; L VLPFC, left ventrolateral prefrontal cortex; L TLant, left temporal lateral anterior cortex; R TLpost, right temporal lateral posterior cortex; R PMM, right premotor medial cortex; R IPL, right inferior parietal lobule.

extensive EZN, some of the sampled brain regions were not involved in the epileptogenic network.

In the present cohort, sampling of subcortical gray matter structures was conducted in all but two patients. The thalamus was the most frequently investigated structure, with sampling available in eight patients. The pulvinar was examined in seven cases, the lateral nucleus in six, the central–lateral nucleus in four, and the mediodorsal nucleus in three. Among the other subcortical structures, the caudate nucleus and putamen were the most sampled (in five cases each), followed by the hypothalamic contacts within and in close proximity to the HH in two patients, and the pallidum in one case. The epileptogenicity profiles of subcortical structures are presented in Figure 3C. In addition to the HH, for which the intrinsic epileptogenicity is well established, the pulvinar and the central–lateral thalamic nuclei were the only structures identified as belonging to the EZN, as delineated by ictal epileptogenicity markers. In contrast, the remaining thalamic nuclei as well as the caudate and putamen demonstrated moderate epileptogenicity, which aligns with the PZN. The pallidum was not implicated in either EZN or PZN, with the finding supported by a single case.

3.4 | Post-SEEG treatments and outcome

Twelve patients (86%) underwent SEEG-guided RF-TC at the end of the SEEG procedure (Table 3). After SEEG-guided RF-TC, six of the 12 patients exhibited a response; five achieved SF for at least 1 month, and three achieved SF for >6 months. One patient who was seizure-free for 11.0 months after RF-TC underwent surgical resection and is currently seizure-free (at follow-up 1.5 years after the surgery; Figure 2). Another patient has been seizure-free for 10.0 months after RF-TC so far. The other patient with an extensive right hemispheric EZN became seizure-free for 12.0 months after 58 contacts were coagulated. The number of brain regions included in the EZN or PZN and the number of RF-TC contacts did not differ significantly between RF-TC responders and nonresponders.

Four patients (29%) underwent curative surgery, and all had visible lesions on MRI, including two FCDs, one polymicrogyria, and one HH. The type of surgery, site of resection, and pathological diagnosis are shown in Table 3. One patient with FCD achieved Engel class I, confirmed at last follow-up 1.5 years postoperatively. Another patient with FCD was initially seizure-free; however, the patient experienced a relapse at 9.0 months postoperatively, corresponding to Engel class II at 1.0 year. The patient with polymicrogyria exhibited worthwhile improvement (Engel class III at 6.0 years), whereas the patient with HH showed no improvement (Engel class IV at 7.0 years).

Two patients underwent radiosurgical anterior two-thirds callosotomy, eight underwent VNS, and one underwent DBS (thalamic pulvinar nucleus). Of the eight patients who underwent VNS, three were classified as responders, with a reduction in seizure frequency of >50%. In contrast, none of the patients who underwent callosotomy or DBS responded.

4 | DISCUSSION

Surgical treatment of LGS is a rare opportunity. Several case reports and studies have indicated that surgical intervention can result in successful outcomes in terms of

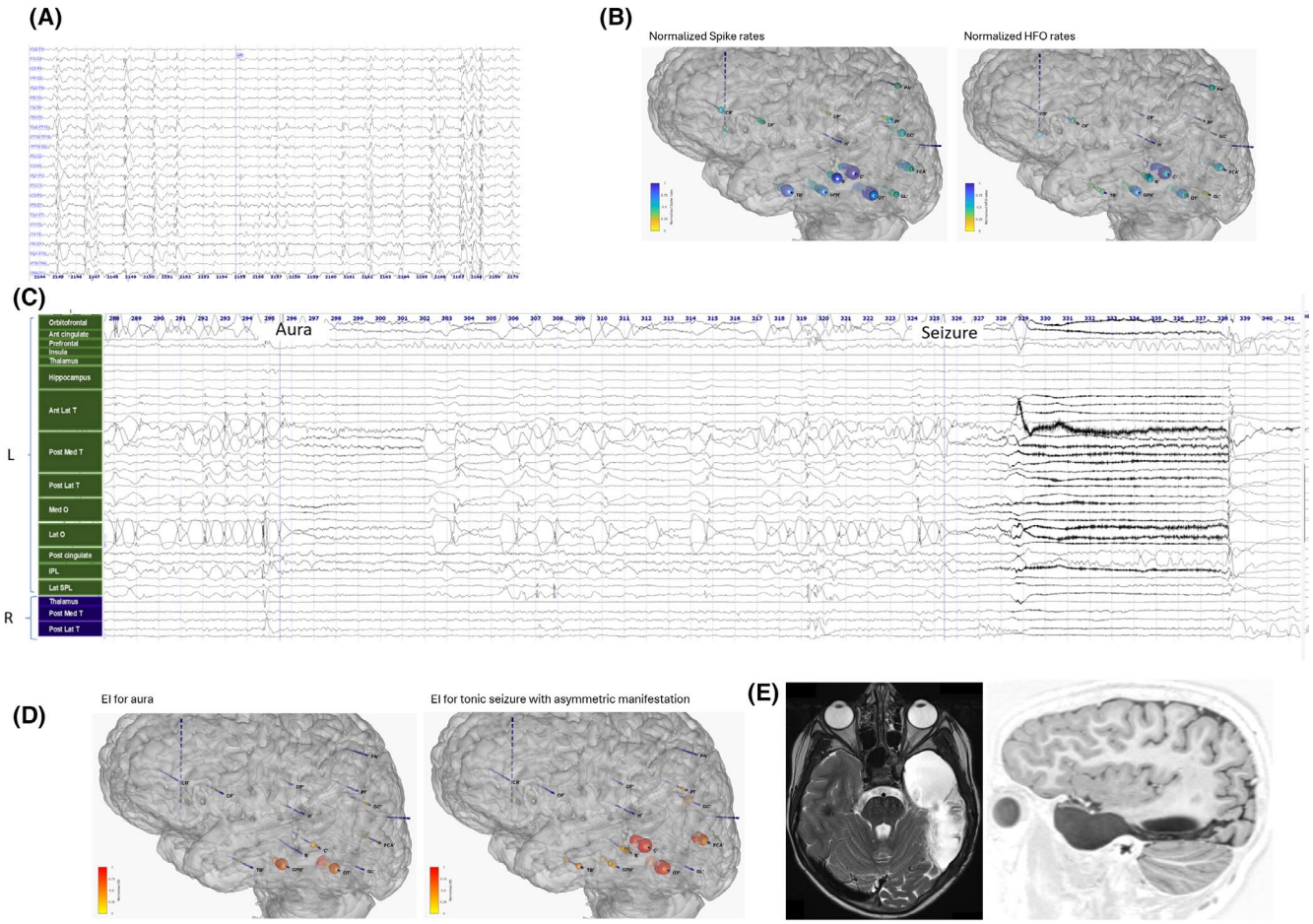

FIGURE 2 An illustrative case of Lennox–Gastaut syndrome with Engel class I surgical outcome (Patient 11). (A) Generalized slow spike-and-wave complexes and repetitive left temporal spikes on interictal scalp electroencephalogram. (B) Quantified interictal stereoelectroencephalographic (SEEG) markers (the maximal normalized spike and high-frequency oscillation [HFO] rates) represented by the color (yellow to blue) and size of the spheres on the patient's three-dimensional (3D) brain mesh with SEEG electrodes. (C) SEEG recordings of a habitual aura followed by tonic seizure with asymmetric features. (D) Quantified ictal SEEG markers (the maximal normalized epileptogenicity index [EI] value) of the aura and tonic seizure represented by the color (yellow to red) and size of the spheres on the patient's 3D brain mesh with SEEG electrodes. (E) Brain magnetic resonance imaging after tailored temporal lobectomy extended to the occipitotemporal resection. L PMM, left premotor medial cortex; L DMPFC, left dorsomedial prefrontal cortex; L ACC, left anterior cingulate cortex; L PML, left premotor lateral cortex; L DLPFC, left dorsolateral prefrontal cortex; L INS, left insula; L Thal, left thalamus; L TMant, left temporomedial anterior; R DMPFC, right dorsomedial prefrontal cortex; R PML, right premotor lateral cortex; HH, hypothalamic hamartoma; R OFC, right orbitofrontal cortex; R DMPFC; right dorsomedial prefrontal cortex; R PML, right premotor lateral cortex; R DLPFC, right dorsolateral prefrontal cortex; R SPLlat, right superior parietal lobule lateral; R Thal, right thalamus; R TMant, right temporomedial anterior cortex; R DLPFC, right dorsolateral prefrontal cortex; L VLPFC, left ventrolateral prefrontal cortex; L TLant, left temporal lateral anterior cortex; R TLpost, right temporal lateral posterior cortex; R PMM, right premotor medial cortex; R IPL, right inferior parietal lobule.

seizure reduction or cessation of cognitive deterioration in patients with LGS with or without MRI lesions.[4–9] In some studies, intracerebral exploration has been proposed as a presurgical strategy when noninvasive investigations suggest a focal etiology.[9,28] The nature of the underlying pathology, the presence of a focal lesion on MRI, concordance of preoperative investigations, the type of surgery, and the duration of epilepsy before surgery have been identified as prognostic factors in postoperative outcome.[7,9,29]

4.1 | Overview of indications and outcome after SEEG

To our knowledge, no series of SEEG-recorded LGS has been published. The indication for SEEG in drug-resistant epilepsy patients with a phenotype of LGS was rare in our experience. Only 14 cases were identified in our cohort of >500 patients, representing <3% of the total cases.

A distributed epileptogenic network was identified in the studied patients. In line with this finding, few

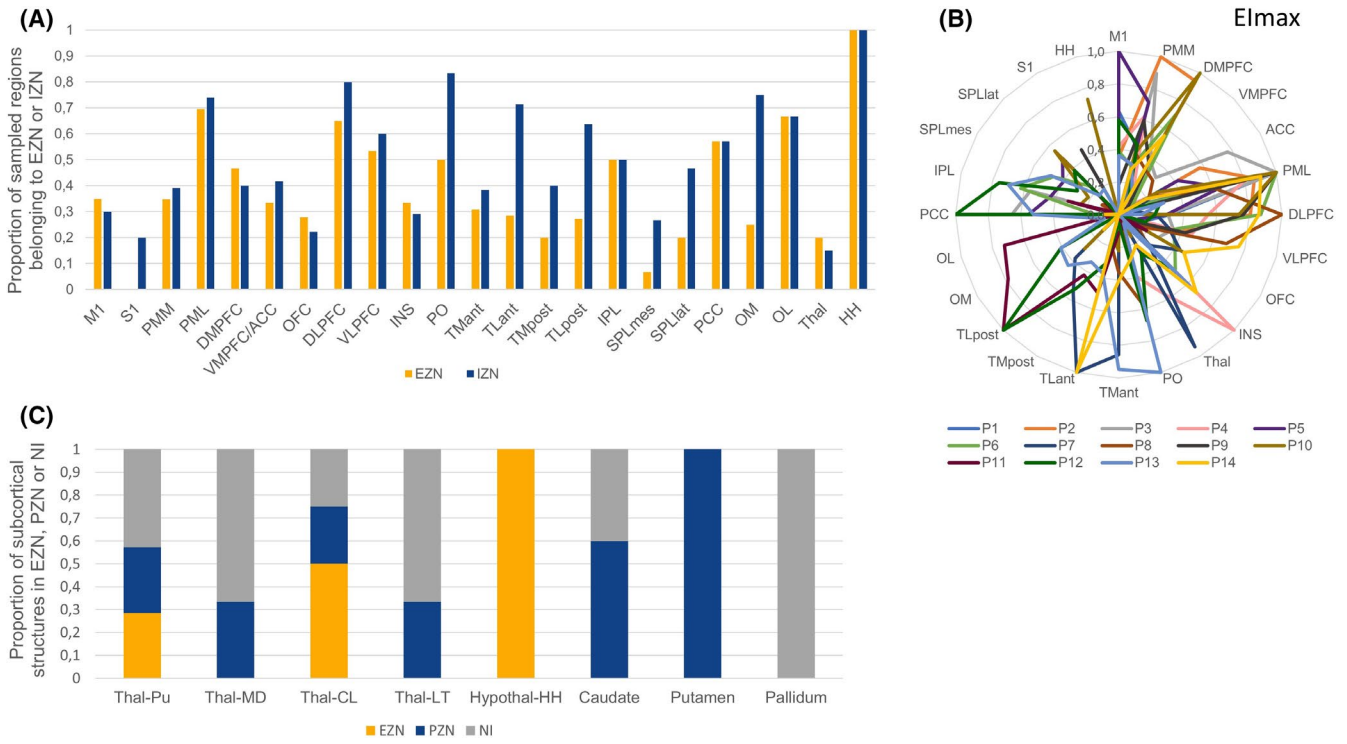

FIGURE 3 (A, B) Epileptogenicity profiles of cortical and subcortical brain regions in Lennox–Gastaut syndrome (LGS) patients at the group level (A) and individual level (B). (A) The number of times each brain region participated in the epileptogenic zone network (EZN; orange) and the irritative zone network (IZN; blue) was controlled for by the number of times each structure was sampled. (B) The individual epileptogenicity profiles of LGS patients were represented by the maximum values of the epileptogenicity index (EImax) per region. (C) The proportion of sampled subcortical structures within the EZN or propagation zone network (PZN) or that were noninvolved (NI). ACC, anterior cingulate cortex; CL, central–lateral nucleus; DLPFC, dorsolateral prefrontal cortex; DMPFC, dorsomedial prefrontal cortex; HH, hypothalamic hamartoma; Hypothal, hypothalamus; INS, insula; IPL, inferior parietal lobule; LT, lateral nucleus; M1, primary motor; MD, mediodorsal nucleus; OFC, orbitofrontal cortex; OL, occipital lateral; OM, occipital mesial; PCC, posterior cingulate cortex; PML, premotor lateral; PMM, premotor mesial; PO, parietal operculum; Pu, pulvinar; S1, primary sensory; SPLlat, superior parietal lobule lateral; SPLmes, superior parietal lobule mesial; Thal, thalamus; TLant, temporal lateral anterior; TLpost, temporal lateral posterior; TMant, temporal mesial anterior; TMpost, temporal mesial posterior; VLPFC, ventrolateral prefrontal cortex; VMPFC, ventromesial prefrontal cortex.

patients underwent curative surgery after SEEG compared to patients with other medically intractable focal epilepsies according to the literature.[27,30,31] In our study, four of 14 patients underwent curative surgery for a localized EZN associated with an epileptogenic lesion. Two cases demonstrated a favorable prognosis (Engel classes I and II) following tailored resective surgery. One case was improved (Engel class III), whereas one case with a previously operated on HH showed no improvement. It should be noted that all cases finally operated on showed a lesion on MRI and positive histopathology. This proves that some well-selected lesional cases could benefit from a surgical resection tailored based on SEEG recordings, even if they are rare. Our study suggests that LGS patients without MRI-visible lesions are less likely to present with a localized EZ.

In this study, six of the 12 patients responded to SEEG-guided RF-TC, and three became seizure-free for >10 months. Given the high seizure burden in LGS patients, this finding may suggest the potential value of RF-TC as a treatment option. This aligns with a recent case report[15] and may also justify the indication of an invasive and potentially risky procedure such as SEEG in this context. Quantifying EZN using ictal epileptogenicity markers, the EI and cEI, may help determine the RF-TC targets.

4.2 | Epileptogenic networks in LGS

SEEG analysis revealed some common features in the SOP and the organization of the epileptogenic network in LGS patients. Most tonic seizures are initiated with LVFA, whereas a slow rhythmic spike–wave discharge is observed in atypical absences. This is consistent with the well-known observations on scalp ictal EEG indicating that the SOPs of tonic seizures and atypical absences are characterized by generalized fast activity and bilateral rhythmic slow spike–waves, respectively.[32,33]

TABLE 3 Post-SEEG treatment outcomes of the patients.

Patient	RF-TC	RF-TC contacts, *n*	SF duration after RF-TC, months	RF-TC, responder, yes/no	Curative surgery/type/pathology	Surgical outcome (Engel class)/duration of postoperative follow-up, years	Callosotomy responder, yes/no	VNS responder, yes/no	DBS, responder, yes/no
P1	No	NA	NA	NA	No	NA	No	No	NA
P2	No	NA	NA	NA	No	NA	NA	NA	NA
P3	Yes	5	.0	Yes	Yes/partial endoscopic ablation (1st, before SEEG) and disconnection of HH (2nd and 3rd)/NA	Engel IV/7.0	NA	No	NA
P4	Yes	41	.0	No	No	NA	No	No	No
P5	Yes	8	.0	No	No	NA	NA	No	NA
P6	Yes	14	.0	No	No	NA	NA	Yes	NA
P7	Yes	16	.0	Yes	Yes/tailored temporal lobe resection, R/FCD IIb	Engel III/6.0	NA	NA	NA
P8	Yes	12	1.0	No	No	NA	NA	No	NA
P9	Yes	35	.0	No	No	NA	NA	Yes	NA
P10	Yes	2	.0	No	No	NA	NA	Yes	NA
P11	Yes	27	11.0	Yes	Yes/tailored temporal lobe resection, L/FCD Ic	Engel I/1.5	NA	NA	NA
P12	Yes	58	12.0	Yes	No	NA	NA	NA	NA
P13	Yes	65	1.5	Yes	Yes/temporoparietal cortectomy, L/polymicrogyria	Engel II/1.0	NA	NA	NA
P14	Yes	13	10.0	Yes	No	NA	NA	NA	NA

Abbreviations: DBS, deep brain stimulation; FCD, focal cortical dysplasia; HH, hypothalamic hamartoma; L, left; NA, not applicable; R, right; RF-TC, radiofrequency thermocoagulation; SEEG, stereoelectroencephalography; SF, seizure freedom; VNS, vagus nerve stimulation.

In this study, the cortical epileptogenic networks of LGS often involved bilateral, multiple brain regions, with prominent involvement of the frontal lobe. Furthermore, the epileptogenic network was observed to frequently involve lateral neocortical structures, particularly premotor–prefrontal–parietal networks, while sparing mesial temporal structures, regardless of the presence, extent, and location of a causative lesion. It has been suggested that the frontal and parietal association cortices may be pivotal regions within the epileptogenic network of generalized seizures.[34] Moreover, activation of the association network has been linked to the occurrence of tonic seizures and GPFA in LGS, which is line with our findings.[35–37] It is important to note that even a widely distributed network did not encompass the entirety of the brain but rather preserved some regions. Although diffuse and generalized interictal abnormalities are observed on the scalp EEG in LGS, not all brain regions are involved.

At the individual level, the epileptogenic networks showed high intersubject variability in their distribution and involvement of brain regions. It has been proposed that common electroclinical features observed in LGS patients with different etiologies may arise from "secondary generalization" involving common cerebral networks.[33,35,38] Subcortical structures may significantly contribute to secondary generalization, as suggested by a previous study.[33] Interactions between cortical and subcortical structures may be implicated in secondary generalization, with the thalamus serving as a key region in this process.[33,39] In this study, a small proportion among the patients with available thalamic sampling (3/8) showed thalamic involvement in the EZN. Regarding the pulvinar, this finding was comparable to that observed in a previous study on focal epilepsies.[40] Involvement of other thalamic nuclei cannot be excluded; in particular, the centromedian nucleus has been shown to play a role in LGS-associated ictal networks and has been suggested as a potential target for DBS in LGS.[39,41,42] The present study further confirmed the high epileptogenicity of HH in epilepsy with HH manifested as LGS. Regarding the basal ganglia, our results highlight the role of the caudate nucleus and the putamen as the nodes of the propagation network in LGS.

LGS is one of the earliest described epileptic syndromes.[1,43] Nevertheless, considerable heterogeneity exists within LGS, which introduces some ambiguity regarding the diagnosis of a single disease entity. Ohtahara et al. divided patients with LGS into typical and atypical cases and noted that the atypical cases might transition from or into other epilepsies, including "partial epilepsy with secondary bilateral synchrony."[44] One research group even employed the term "Lennox–Gastaut phenotype" to describe patients exhibiting the majority of the electroclinical characteristics of LGS (tonic seizures, SSW, and GPFA) while also displaying some atypical features (e.g., an older age at onset or minimal to mild intellectual disability).[33] Subclassification of LGS may be possible if a sufficiently large number of LGS patients with focal and localized epileptogenic networks, as assessed by SEEG, are collected and their characteristics studied.

4.3 | Limitations of the study

It is important to acknowledge the potential for bias and the limitations of the study. First, the sampling limitations of the SEEG method represent a known source of bias. Nevertheless, SEEG is the only electrophysiological technique that can simultaneously sample cortical and subcortical structures, which is crucial for investigating EZN organization in LGS. The subcortical coverage of SEEG depends on the electrode trajectories, which primarily target cortical structures according to the individual hypothesis regarding the EZN, as well as some thalamic nuclei as potential DBS targets. The number of implanted electrodes is limited to those required for routine clinical care, with careful consideration given to the risks to benefits ratio. Consequently, the thalamic nuclei sampled in the present retrospective study were those available as part of the trajectories, whereas the centromedian nucleus, requiring an additional electrode, was not sampled. Additionally, the small sample size limits the conclusions that can be drawn regarding the involvement of some less frequently explored cortical regions, such as the occipital cortices.

5 | CONCLUSIONS

This study presents the first comprehensive description of patients with LGS explored with SEEG. The epileptogenic networks of LGS were mostly widely distributed and often involved bilateral prefrontal–premotor and parietal regions. However, some carefully selected patients with LGS presenting with evidence of highly localized EZ based on comprehensive noninvasive evaluation may be eligible for SEEG, as are other patients with drug-resistant focal epilepsy. SEEG quantification may offer valuable insights into the decision-making process surrounding resective surgery and/or RF-TC strategies.

AUTHOR CONTRIBUTIONS

Soomi Cho: Data curation; formal analysis; methodology; figures and tables; writing—original draft preparation. **Julia Makhalova:** Data curation; methodology;

figures and tables; supervision; writing—reviewing and editing. **Samuel Medina Villalon:** Methodology; software; writing—reviewing and editing. **Nathalie Villeneuve:** Writing—reviewing and editing. **Agnes Trébuchon:** Writing—reviewing and editing. **Manel Krouma:** Writing—reviewing and editing. **Didier Scavarda:** Writing—reviewing and editing. **Anne Lépine:** Writing—reviewing and editing. **Mathieu Milh:** Writing—reviewing and editing. **Romain Carron:** Writing—reviewing and editing. **Francesca Bonini:** Writing—reviewing and editing. **Géraldine Daquin:** Writing—reviewing and editing. **Sandrine Aubert:** Writing—reviewing and editing. **Stanislas Lagarde:** Methodology; supervision; writing—reviewing and editing. **Francesca Pizzo:** Methodology; supervision; writing—reviewing and editing. **Fabrice Bartolomei:** Conceptualization; investigation; supervision; writing—reviewing and editing.

ACKNOWLEDGMENTS

We thank Bruno Colombet for his technical assistance.

CONFLICT OF INTEREST STATEMENT

None of the authors has any conflict of interest to disclose. We confirm that we have read the Journal's position on issues involved in ethical publication and affirm that this report is consistent with those guidelines.

DATA AVAILABILITY STATEMENT

The data that support the findings of this study are available on request from the corresponding author. The data are not publicly available due to privacy or ethical restrictions.

ORCID

Soomi Cho https://orcid.org/0000-0003-4723-8975
Julia Makhalova https://orcid.org/0000-0001-7962-2942
Didier Scavarda https://orcid.org/0000-0001-9344-8071
Mathieu Milh https://orcid.org/0000-0002-2454-8543
Stanislas Lagarde https://orcid.org/0000-0003-2916-1302
Francesca Pizzo https://orcid.org/0000-0001-6345-1288
Fabrice Bartolomei https://orcid.org/0000-0002-1678-0297

REFERENCES

1. Gastaut H, Roger J, Soulayrol R, Tassinari C, Regis H, Dravet C, et al. Childhood epileptic encephalopathy with diffuse slow spike-waves (otherwise known as "petit mal variant") or Lennox syndrome. Epilepsia. 1966;7:139–79.
2. Arzimanoglou A, French J, Blume WT, Cross JH, Ernst J-P, Feucht M, et al. Lennox-Gastaut syndrome: a consensus approach on diagnosis, assessment, management, and trial methodology. The Lancet Neurol. 2009;8:82–93.
3. Specchio N, Wirrell EC, Scheffer IE, Nabbout R, Riney K, Samia P, et al. International league against epilepsy classification and definition of epilepsy syndromes with onset in childhood: position paper by the ILAE task force on nosology and definitions. Epilepsia. 2022;63:1398–442.
4. Angelini L, Broggi G, Riva D, Solero CL. A case of Lennox-Gastaut syndrome successfully treated by removal of a parieto-temporal astrocytoma. Epilepsia. 1979;20:665–9.
5. Quarato PP, Di Gennaro G, Manfredi M, Esposito V. Atypical Lennox–Gastaut syndrome successfully treated with removal of a parietal dysembryoplastic tumour. Seizure. 2002;11:325–9.
6. You SJ, Lee J-K, Ko T-S. Epilepsy surgery in a patient with Lennox–Gastaut syndrome and cortical dysplasia. Brain and Development. 2007;29:167–70.
7. Liu S-Y, An N, Fang X, Singh P, Oommen J, Yin Q, et al. Surgical treatment of patients with Lennox-Gastaut syndrome phenotype. Sci World J. 2012;2012: 614263.
8. Ding P, Liang S, Zhang S, Zhang J, Hu X, Yu X. Resective surgery combined with corpus callosotomy for children with non-focal lesional Lennox–Gastaut syndrome. Acta Neurochir. 2016;158:2177–84.
9. Kang JW, Eom S, Hong W, Kwon HE, Park S, Ko A, et al. Long-term outcome of resective epilepsy surgery in patients with Lennox-Gastaut syndrome. Pediatrics. 2018;142(4):e20180449. https://doi.org/10.1542/peds.2018-0449
10. Douglass LM, Salpekar J. Surgical options for patients with Lennox-Gastaut syndrome. Epilepsia. 2014;55:21–8.
11. Bartolomei F, Lagarde S, Wendling F, McGonigal A, Jirsa V, Guye M, et al. Defining epileptogenic networks: contribution of SEEG and signal analysis. Epilepsia. 2017;58:1131–47.
12. Jung Y-J, Kang H-C, Choi K-O, Lee JS, Kim D-S, Cho J-H, et al. Localization of ictal onset zones in Lennox-Gastaut syndrome using directional connectivity analysis of intracranial electroencephalography. Seizure. 2011;20:449–57.
13. Kim J-Y, Kang H-C, Kim K, Kim HD, Im C-H. Localization of epileptogenic zones in Lennox–Gastaut syndrome (LGS) using graph theoretical analysis of ictal intracranial EEG: a preliminary investigation. Brain and Development. 2015;37:29–36.
14. Lee D, Liang J, Hur YJ, Kim N-Y, Kim HD. Spectral characteristics of intracranial electroencephalographic activity in patients with Lennox–Gastaut syndrome. Brain and Development. 2017;39:138–44.
15. Li S, Cai X, Yao C, Wang Y, Xiao X, Yang H, et al. Case report: late-onset Lennox-Gastaut syndrome treated with stereotactic electroencephalography-guided radiofrequency thermocoagulation before craniotomy. Front Neurol. 2022;13:857767.
16. Isnard J, Taussig D, Bartolomei F, Bourdillon P, Catenoix H, Chassoux F, et al. French guidelines on stereoelectroencephalography (SEEG). Neurophysiol Clin. 2018;48:5–13.
17. Makhalova J, Medina Villalon S, Wang H, Giusiano B, Woodman M, Bénar C, et al. Virtual epileptic patient brain modeling: relationships with seizure onset and surgical outcome. Epilepsia. 2022;63:1942–55.
18. Colombet B, Woodman M, Badier J, Bénar C. AnyWave: a cross-platform and modular software for visualizing and processing electrophysiological signals. J Neurosci Methods. 2015;242:118–26.

19. Bartolomei F, Chauvel P, Wendling F. Epileptogenicity of brain structures in human temporal lobe epilepsy: a quantified study from intracerebral EEG. Brain. 2008;131:1818–30.
20. Balatskaya A, Roehri N, Lagarde S, Pizzo F, Medina S, Wendling F, et al. The "connectivity epileptogenicity index-"(cEI), a method for mapping the different seizure onset patterns in StereoElectroEncephalography recorded seizures. Clin Neurophysiol. 2020;131:1947–55.
21. Roehri N, Lina J-M, Mosher JC, Bartolomei F, Bénar C-G. Time-frequency strategies for increasing high-frequency oscillation detectability in intracerebral EEG. IEEE Trans Biomed Eng. 2016;63:2595–606.
22. Makhalova J, Madec T, Medina Villalon S, Jegou A, Lagarde S, Carron R, et al. The role of quantitative markers in surgical prognostication after stereoelectroencephalography. Ann Clin Transl Neurol. 2023;10:2114–26.
23. Wang HE, Scholly J, Triebkorn P, Sip V, Medina Villalon S, Woodman MM, et al. Vep atlas: an anatomic and functional human brain atlas dedicated to epilepsy patients.
24. Brun G, Testud B, Girard OM, Lehmann P, de Rochefort L, Besson P, et al. Automatic segmentation of deep grey nuclei using a high-resolution 7T magnetic resonance imaging atlas: quantification of T1 values in healthy volunteers. Eur J Neurosci. 2022;55(2):438–60. https://doi.org/10.1111/ejn.15575
25. Contento M, Pizzo F, López-Madrona VJ, Lagarde S, Makhalova J, Trébuchon A, et al. Changes in epileptogenicity biomarkers after stereotactic thermocoagulation. Epilepsia. 2021;62:2048–59.
26. Simula S, Garnier E, Contento M, Pizzo F, Makhalova J, Lagarde S, et al. Changes in local and network brain activity after stereotactic thermocoagulation in patients with drug-resistant epilepsy. Epilepsia. 2023;64:1582–93.
27. Lagarde S, Buzori S, Trebuchon A, Carron R, Scavarda D, Milh M, et al. The repertoire of seizure onset patterns in human focal epilepsies: determinants and prognostic values. Epilepsia. 2019;60:85–95.
28. Lee YJ, Kang H-C, Lee JS, Kim SH, Kim D-S, Shim K-W, et al. Resective pediatric epilepsy surgery in Lennox-Gastaut syndrome. Pediatrics. 2010;125:e58–e66.
29. Liu Q, Wu N, Liu C, Yu H, Sun Y, Wang Y, et al. Pediatric epilepsy surgery in patients with Lennox-Gastaut syndrome after viral encephalitis. Front Neurol. 2023;14:1097535.
30. Cardinale F, Rizzi M, Vignati E, Cossu M, Castana L, d'Orio P, et al. Stereoelectroencephalography: retrospective analysis of 742 procedures in a single centre. Brain. 2019;142:2688–704.
31. Steriade C, Martins W, Bulacio J, Morita-Sherman ME, Nair D, Gupta A, et al. Localization yield and seizure outcome in patients undergoing bilateral SEEG exploration. Epilepsia. 2019;60:107–20.
32. Roger J, Fau-Dravet C, Bureau M. The Lennox-Gastaut Syndrome. Cleve Clin J Med. 1989;56(Suppl Pt 2):S172-80
33. Archer JS, Warren AE, Jackson GD, Abbott DF. Conceptualizing Lennox–Gastaut syndrome as a secondary network epilepsy Frontiers in neurology. 2014;5:104270.
34. Blumenfeld H, Westerveld M, Ostroff RB, Vanderhill SD, Freeman J, Necochea A, et al. Selective frontal, parietal, and temporal networks in generalized seizures. NeuroImage. 2003;19:1556–66.
35. Pillay N, Archer JS, Badawy RA, Flanagan DF, Berkovic SF, Jackson G. Networks underlying paroxysmal fast activity and slow spike and wave in Lennox-Gastaut syndrome. Neurology. 2013;81:665–73.
36. Intusoma U, Abbott DF, Masterton RA, Stagnitti MR, Newton MR, Jackson GD, et al. Tonic seizures of Lennox-Gastaut syndrome: periictal single-photon emission computed tomography suggests a corticopontine network. Epilepsia. 2013;54:2151–7.
37. Archer JS, Warren AE, Stagnitti MR, Masterton RA, Abbott DF, Jackson GD. Lennox-Gastaut syndrome and phenotype: secondary network epilepsies. Epilepsia. 2014;55:1245–54.
38. Warren AE, Abbott DF, Vaughan DN, Jackson GD, Archer JS. Abnormal cognitive network interactions in Lennox-Gastaut syndrome: a potential mechanism of epileptic encephalopathy. Epilepsia. 2016;57:812–22.
39. Dalic LJ, Warren AE, Young JC, Thevathasan W, Roten A, Bulluss KJ, et al. Cortex leads the thalamic centromedian nucleus in generalized epileptic discharges in Lennox-Gastaut syndrome. Epilepsia. 2020;61:2214–23.
40. Pizzo F, Roehri N, Giusiano B, Lagarde S, Carron R, Scavarda D, et al. The ictal signature of thalamus and basal ganglia in focal epilepsy: a SEEG study. Neurology. 2021;96:e280–e293.
41. Shlobin NA, Hofmann K, Cohen NT, Koubeissi MZ, Gaillard WD, Oluigbo CO. Deep brain stimulation of the centromedian nucleus of the thalamus for Lennox-Gastaut syndrome: a systematic review and individual patient data analysis. Neurosurgery. 2023;92:703–15.
42. Dalic LJ, Warren AE, Bulluss KJ, Thevathasan W, Roten A, Churilov L, et al. DBS of thalamic centromedian nucleus for Lennox–Gastaut syndrome (ESTEL trial) annals of neurology. 2022;91:253–67.
43. Epilepsy CoCaTotILA. Proposal for revised classification of epilepsies and epileptic syndromes. Epilepsia. 1989;30:389–99.
44. Ohtahara S, Ohtsuka Y, Kobayashi K. Lennox-Gastaut syndrome: a new vista. Psychiatry Clin Neurosci. 1995;49:S179–S183.

SUPPORTING INFORMATION

Additional supporting information can be found online in the Supporting Information section at the end of this article.

How to cite this article: Cho S, Makhalova J, Medina Villalon S, Villeneuve N, Trébuchon A, Krouma M, et al. Stereoelectroencephalographic exploration and surgical outcome in Lennox–Gastaut syndrome. Epilepsia. 2025;66:1417–1432. https://doi.org/10.1111/epi.18283